Electrical conductivity of dense copper and aluminum plasmas

A. W. DeSilva and J. D. Katsouros
Laboratory for Plasma Research and Department of Physics, University of Maryland at College Park, College Park, Maryland 20742
(Received 10 November 1997)

Measurements are reported of the electrical conductivity of dense copper and aluminum plasmas in the temperature range 10–30 kK, in a density range from about one-fifth solid density down to 0.02 g/cm^3. Plasmas were created by rapid vaporization of metal wires in a water bath. At temperatures below about 15 kK, as density decreases from the highest values measured, the conductivity falls roughly as the cube of density, reaches a minimum, and subsequently rises to approach the Spitzer prediction at low density. This minimum is not seen for temperatures above about 20 kK. These results are compared with several theoretical predictions. [S1063-651X(98)05305-7]

PACS number(s): 52.25.Fi, 52.80.Mg, 52.80.Qj

I. INTRODUCTION

In a previous paper [1] (referred to as I), we presented measurements of the electrical conductivity of copper plasmas having densities ranging from about 0.3 to 3 g/cm^3, and temperatures in the range 8000–30 000 K. Data for that report were obtained by measuring the resistance of plasma created by vaporizing copper wires inside glass capillaries. We showed that, for values of the coupling parameter Γ ($\Gamma = Z^2e^2/akT$, $4\pi a^3/3 = ni^{-1}$) ranging from about 10 to 100, the conductivity appeared to become a function of Γ alone.

In the present paper, we have extended these measurements to lower densities and smaller values of Γ, and show that the simple dependence on Γ shown in I breaks down. We have departed in the present work from the use of glass capillaries to confine the plasma during the brief measurement period, and have instead utilized water as the confining medium for the vaporized metal wires, a method that offers a significant advantage in interpretation, while restricting somewhat the high density limit of measurement.

In order to make a measurement of the dc electrical conductivity of a plasma, we create a cylindrical plasma by vaporizing, with a burst of current, a metal wire embedded in water. The resulting plasma column expands radially, compressing the surrounding water and causing a cylindrical shock wave to move radially outwards in the water. The plasma is observed to remain quite stable during this expansion, and very little diffusion of energy occurs between the plasma and water on the short time scale of the observation. Determination of the resistance of the column is straightforward, as both the current and voltage across the column may be measured. The voltage across the plasma consists of the pure resistive part that results from the plasma conductivity, and a reactive part due to the time-varying inductance of the column and to the time-changing current. Subtracting these reactive components from the measured voltage, we are left with the real resistance of the column. To deduce the conductivity, we need only know the column diameter, which is observable photographically, and its length, which is assumed constant during the interval of measurement.

II. EXPERIMENTAL SETUP

The discharge chamber (Fig. 1) is an aluminum cylinder 30 cm in diameter and 15 cm in height. The electrode through which current is introduced enters coaxially from the bottom, and the load wire is stretched between this electrode and a grounded support positioned 26 mm above the electrode. Current return from the top of the wire takes place through four rods positioned symmetrically about the wire. The chamber is fitted with four windows, placed 90° apart, to allow optical observation of the plasma. After a load wire has been installed, the chamber is filled with deionized water.

Current is driven from a pair of capacitors connected in parallel, totaling 3.86 μF. The rated voltage of these capacitors is 60 kV, although they have been used in this work only up to about 25 kV. Current is switched by a pressurized sparkgap switch. The inductance of the circuit, exclusive of the wire load, is about 230 nH. Additional inductance or series resistance may easily be inserted into the circuit, giving a degree of control over the current wave form. We have also used a fusible link in parallel with the resistor, which gives additional control over the current wave form reaching the test wire. A Rogowski belt surrounds the main electrode to measure the time derivative of the current, and a voltage divider, consisting of a 120-Ω resistor (six 20-Ω 2-W carbon resistors in series) in series with a 1-Ω resistor, is used to measure voltage at the load. The 1-Ω resistor consists of six parallel 6.2-Ω resistors, mounted in a low inductance configuration.

Circuit parameters may be measured by installing a cylindrical plug in place of the wire load, and firing. Such a load is essentially purely inductive, and it is from the observed ringing period that the bank inductance is determined. Voltage and current may be recorded for this inductive load, and subsequent comparison of $V(t)$ with $dI(t)/dt$ serves to confirm that the diagnostics are functioning correctly.

Light from the plasma is focused on a slit oriented perpendicular to the wire, which passes this image to a rotating mirror streak camera that records the time history of the plasma column diameter at 2:1 magnification. A xenon flashlamp is used to backlight the wire, making the plasma column visible in silhouette. The writing speed of the camera

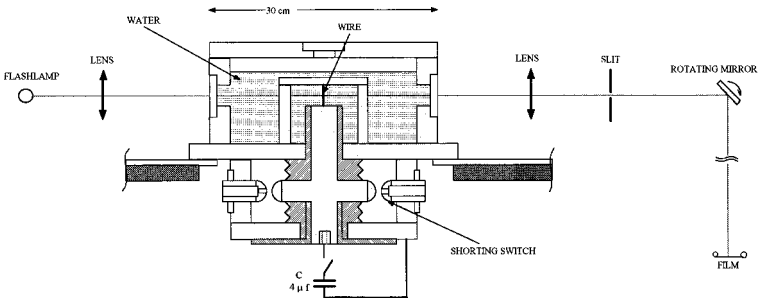

FIG. 1. Cross section through a diameter of the discharge chamber. The short-circuiting switch (crowbar) was not used in this work.

is 6.76 mm/μs, which was determined from careful measurements of the rotation speed of the rotating mirror. In order to fix the time of the streak relative to that of the electrical signals recorded on the digital oscilloscope, a small spark that could be seen by the streak camera was produced by a high voltage pulser. The electrical signal from the pulser was also recorded on the oscilloscope, giving us an absolute synchronization of the times of optical and electrical data. Figure 2 shows a typical streak picture. The shock wave propagating through the water is clearly visible, since the density gradient at the shockfront strongly refracts the backlight. The plasma itself is opaque to the backlight, and is also easily seen. The plasma is sufficiently self-luminous at early times to show up on the film as a light burst near the start of expansion. It is also possible on original photographs to make out a weak shock wave that precedes the main shock. This is due to the expansion that occurs as the wire passes from a solid to a liquid state. This picture demonstrates one of the great advantages of using water as a confining medium, over the use of glass capillaries. In the case of a capillary, the shock wave fractures the glass immediately behind the shockfront, making direct observation of the plasma column impossible. Using water, we can observe the column diameter as a function of time, which we need to determine the plasma density and to calculate the conductivity. In addition, the plasma density is measurable at all relevant times in the water case, while, in the case of glass capillaries, there is a short period as the wire vaporizes when the vapor has not yet filled the tube uniformly, leading to an uncertainty in the density for these times.

III. DATA ANALYSIS

In interpreting the data, we assume a uniformity of the plasma column. To support this assumption we estimate the

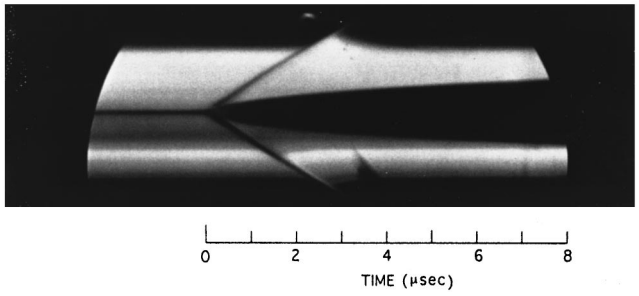

FIG. 2. Typical streak photo. The time axis runs horizontally. The shock wave is identified as the two diverging lines that originate at $t=0$, and the dark shadow is the plasma. The light output of the xenon lamp is somewhat nonuniform, resulting in the variations in the backlight intensity perpendicular to the time axis. Apparent asymmetries are due to diffractive effects from nonuniform backlighting. The time reference spark is visible at top at 2.3 μsec.

thickness Δr of the boundary layer that forms at the interface between water and plasma. A scale length for the thickness Δr of this boundary layer is obtained by equating the heat flow in the temperature gradient across the layer to that required to raise the temperature of a layer of that thickness in a time Δt. The result is

$$\Delta r^2=\frac{\lambda \Delta t}{\rho_m C}, \tag{1}$$

where λ is the thermal conductivity, ρ_m is the mass density, and C is the specific heat. Inserting parameters appropriate for water, utilizing the thermal conductivity for compressed heated water [2], and taking for the time scale an observation time of about 1 μs, we find the scale length for the boundary layer thickness to be about 1 μm. Applying the same formula to the parameters appropriate to the plasma, utilizing the Wiedemann-Franz relation to deduce the thermal conductivity from our measured electrical conductivity, we find that the scale thickness of the boundary layer is about 2 μm. Since wires are 50–250 μm in diameter and the plasma column grows in diameter, we conclude that boundary layer at the plasma-water interface is thin enough to be ignored in our calculations of the conductivity.

The axial uniformity of the plasma column has been checked by making framing camera photographs of the expanding plasma at 5-ns exposure time. No rippling of the plasma surface was visible down to the resolution limit of about 80 μm.

For each shot, we record dI/dt (the time derivative of the current I) and the voltage across the plasma at 5-ns sampling intervals, and a streak camera picture of the expanding plasma. dI/dt is numerically integrated to obtain $I(t)$, or may be determined from passive integration of the current derivative. We have confirmed that the two methods give closely similar results. The recorded voltage is $V=IR+LdI/dt+IdL/dt$. Reactive contributions represented by the two last terms on the right must be subtracted out in order to obtain the true Ohmic potential drop V_R across the column, and R is then the ratio V_R/I. As both of the reactive terms are time dependent, we analyze the data for each 5-ns time step. Time profiles of I and V_R for a typical shot are shown in Fig. 3(a).

Up to the point when the temperature of the wire reaches about 1000 K, the energy input Δe to the wire at each step is calculated from $I^2R\Delta t$, where $R(T)$ is determined from published data for the resistivity of the solid or liquid metal [3]. Above that temperature, the energy input is determined from the product $V_RI\Delta t$, where V_R is the measured voltage less the computed reactive contributions. The change in tempera-

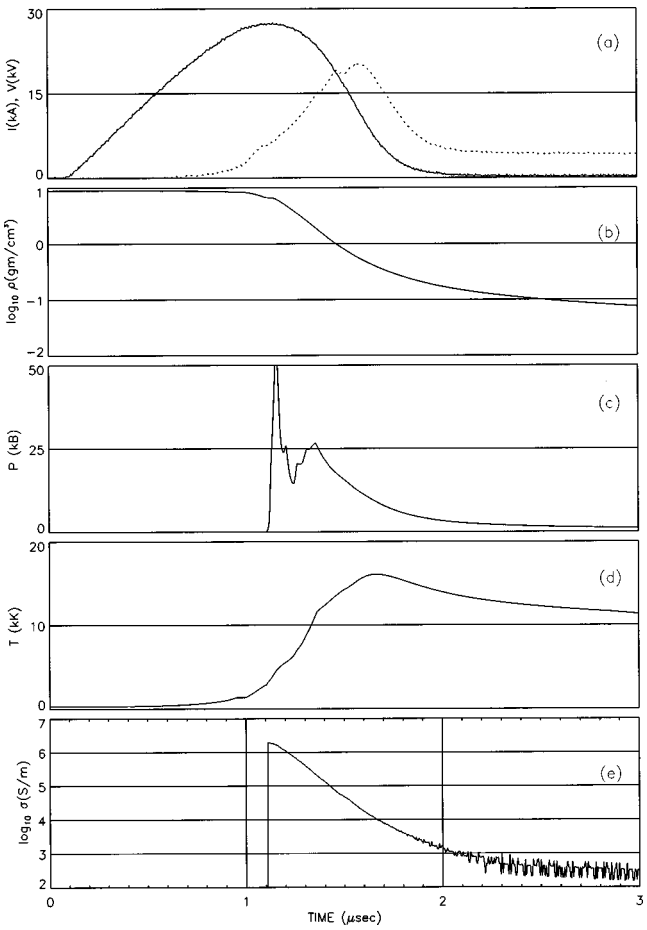

FIG. 3. (a) Measured time traces of current (solid line) and Ohmic voltage (dotted line). (b)–(e) Computed time traces of (b) mass density, (c) pressure, (d) temperature, and (e) conductivity. Data up to only 2μs were retained for this shot.

ture is computed using tabulated data for the specific heat of the metal [4]. Tabulated data for the temperature dependence of density in both solid and liquid states [5,6] are also used to determine the radial expansion of the wire, from which the rate of change in inductance is calculated. Although in principal the energy input could be determined throughout from the measured voltage and current using $\Delta e = V_R I \Delta t$, less error is incurred in the early stages, when the resistance is very small, through use of tabulated resistivity to obtain energy input from I^2R. For the first few dozen time steps, the resistance of the wire and dL/dt are both small enough that the IR and IdL/dt terms are negligible relative to the LdI/dt term, and the wire inductance L may be determined as the ratio of voltage to the current time derivative. This checks well with the inductance computed from handbook formulas. After the temperature of the wire reaches 1000 K, the resistance of the wire has risen enough that we may switch to computing energy input to the wire from $V_R I \Delta t$. In this manner the state of the wire is followed until the temperature reaches the vaporization temperature (2863 K for Cu, 1332 K for Al). At this point, the pressure on the wire may be considerably above 1 bar, since the expansion occurring on melting already sends a compression wave into the water, with the result that the vaporization temperature will be higher than the normal melting temperature.

As the wire vaporizes, the pressure rises rapidly, and the surrounding water is compressed, sending a shock wave radially outwards, as may be seen in Fig. 2. The density of the plasma as a function of time may be determined from observation of the streak photo, making use of the assumption that the mass of wire initially present now fills the plasma volume uniformly, and ignoring any edge effects. Then the conductivity follows simply from

$$\sigma = \frac{1}{RA}, \tag{2}$$

where A is the cross-sectional area of the column.

A satisfactory method to measure the plasma temperature has not been found. Owing to the high plasma density, the optical depth is very small, on the order of μm, so one would expect that light radiated from the plasma would be Planckian, but representative of the plasma at a depth that lies only in the boundary layer. Therefore, a measurement of the absolute radiation intensity would be characteristic only of some region in the transition layer from hot plasma to cold water, and not of the bulk of the plasma. We are forced, therefore, to use an indirect means of finding the temperature.

To do this, we make use of the LANL SESAME equation of state tables [7] for the metal under study to relate the measured input energy to the column to the changes in temperature and pressure. We need, in addition, a model for the growth of the column diameter due to the plasma pressure. A one-dimensional cylindrical fluid code, following the model of Plooster [8], is used to describe the compression wave that propagates into the water. It shows the compression of the water by the expanding copper vapor, and the shock wave generated by this compression. The equation of state data of water for use in this code are taken from Rice and Walsh [9].

We calculate the energy input $V_R I \Delta t$ to the plasma for each 5-ns recorded time step. From the SESAME tables, this is used to find the pressure rise at constant volume. The new pressure is then used to drive the water compression model through a single time step. The resultant plasma expansion yields a new copper density, and the SESAME tables are consulted again to make an adiabatic expansion to the new density, resulting in modified temperature and pressure. Thus, for a single time step, the plasma is assumed to undergo an isochoric addition of energy, followed by an adiabatic expansion. This procedure is used step by step to produce time profiles of the plasma, density, pressure, and temperature. Figures 3(b)–3(d) show the results of this calculation for the shot of Fig. 2.

The spike in pressure as the pressure first rises is an artifact due to the granularity of the SESAME table, in which the pressure changes by several orders in a single density step at the point where vaporization occurs. The spike is narrow enough that it has little effect on the subsequent water dynamics.

Once these parameters are found, it is a simple matter to compute the conductivity σ of the copper column. Figure Fig. 3(e) shows the resulting time history of conductivity. The plasma column diameter computed as above may be compared with the column diameter observed by streak pho-

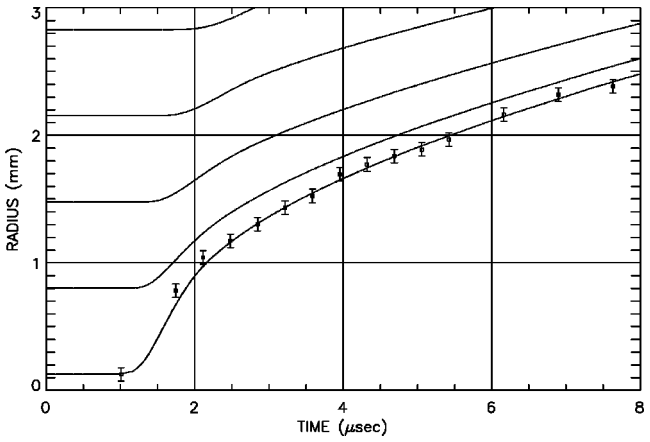

FIG. 4. Comparison of computed plasma radius with streak picture, for the shot of Fig. 2. The solid lines are loci of the first five grid radii from the code. Error bars on measured points indicate an estimate of error in reading radius from the photo.

tography. Figure 4 shows this comparison for the shot pictured in Fig. 2. The time correspondence for this comparison was made using the spark marker described above, thus there are no adjustable parameters. The close correspondence between calculated and observed diameters gives confidence that the calculations yield a valid picture of the plasma expansion and the temperature.

The plasma density is computed by dividing the known mass of the wire by the plasma volume, which is obtained either from streak photographs or from the modeled calculation. As the plasma column expands due to the high internal pressure, the density falls, providing us with a simple means to measure conductivities at a variety of densities. Variation of the charge voltage on the capacitor and of the external series impedance in the circuit allows some control over the temperature versus density profile.

A problem occurs in making measurements at the lowest temperatures and at low density. As the wire reaches the plasma state, the resistance rises dramatically, which tends to diminish the current through the plasma strongly. However, the current must be maintained at some minimum level in order to make the resistance measurement. If the capacitor bank voltage is set too low, the current becomes uselessly small. If the voltage is too high, the current first drops as with a low voltage shot, but then greatly increases, heating the plasma. Use of a fixed external resistance in the circuit tends to decouple the current from the fluctuations in sample resistance, allowing us to obtain late time measurements. We have also employed a modified circuit featuring a relatively large fixed series resistor ($10\ \Omega$) in parallel with a fuse. The fuse is a 6-in. length of copper wire embedded in damp sand. Its resistance remains low as the specimen wire heats and turns to plasma, but then rapidly increases and the fuse opens. Therefore, just as the specimen plasma resistance becomes low, the circuit resistance rises, tending to maintain a small current through the plasma large enough for measurement, but small enough to limit heating.

IV. RESULTS

A. Copper

Several hundred shots were made, using 99.9% purity 125-μm diameter copper wire as the specimen, and using a variety of charge voltages and external series impedances in the discharge circuit. For each shot, the time history of the measured and calculated parameters were recorded. Data at times when the calculated temperature was within $\pm 3\%$ of selected temperatures (in 2000-K steps) were then extracted for plotting in Fig. 5.

For a temperature of 10 000 K, as shown in Fig. 5(a), one sees that, as density decreases, the conductivity falls steeply, varying at the highest densities approximately as ρ^3 with

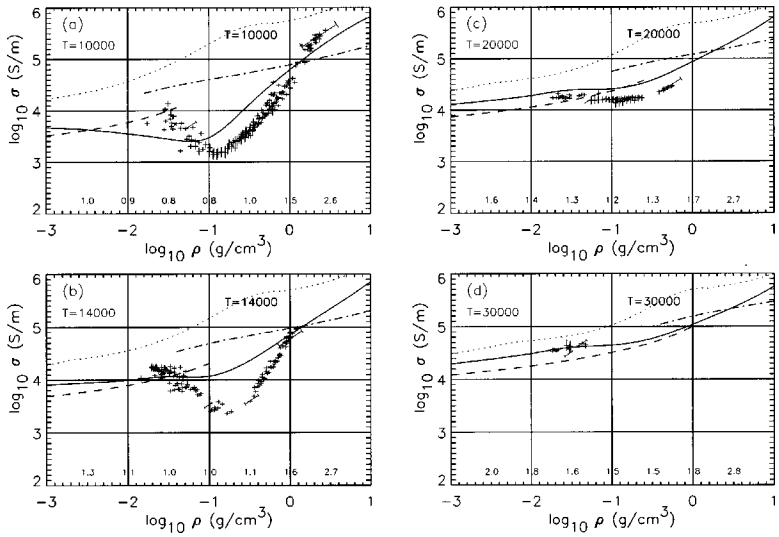

FIG. 5. Electrical conductivity of copper plasma at four temperatures. Crosses represent the estimated error due to current and voltage measurements, and slanted lines on selected points show estimated error due to uncertainty in column radius (see text). Theoretical curves are from Ebeling *et al.* [16] (solid line), Lee and More [17] (dotted line), Ichimaru and Tanaka [18] (dashed line), and Kurilenkov and Valuev [19] (dashed-dotted line). Plots of the first two theories embody variations in Z, while the latter two theories are for the case $Z=1$. We use the Thomas-Fermi model of More [12] to estimate the Z of our plasmas. Numbers at the bottom of the plots show Z variation with density from this model.

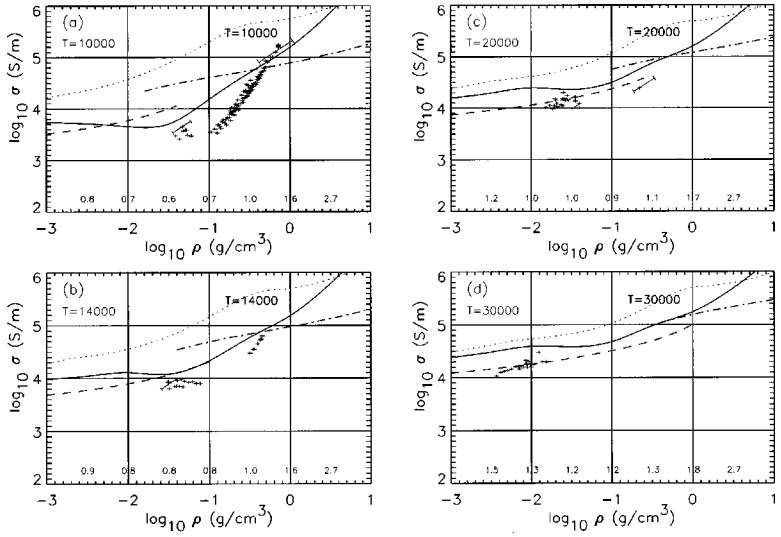

FIG. 6. Electrical conductivity of aluminum plasma at four temperatures. The theory curves are as in Fig. 5.

density. At about 0.1g/cm^3, conductivity goes through a minimum and subsequently rises with falling density. Such behavior has been predicted in dense hydrogen plasmas by Reinholz, Redemer, and Nagel [10], and has been seen in measurements on mercury plasmas [11]. The conductivity must rise from the minimum as density falls if it is to connect at very low density with the Spitzer formula. For higher temperatures [Figs. 5(b)–5(d)], the minimum becomes less pronounced, and, at a temperature of 20 kK, disappears entirely. At the higher temperatures, it was not possible to record data at the highest densities, since expansion is occurring even as the plasma heats. Water is less effective in impeding expansion of the plasma than was the glass capillary used in earlier work. The higher density and lower compressibility of glass accounts for the success in those cases of making observations at high plasma pressures. The observations reported here, however, extend to lower densities than those reported in I. We have been able, using this technique, to record conductivities for densities down to about 0.01 g/cm^3.

B. Aluminum

A similar set of data were taken with 99.9% pure aluminum wires. Resultant conductivity data are shown in Fig. 6. Due to the lower mass density of aluminum, the curves of conductivity versus density are shifted to the left compared to those of copper. Otherwise, quite similar behavior is seen. The data for the two metals are almost identical, within the errors, if plotted versus electron density, or versus the coupling constant Γ. In Fig. 7, we display the data for both aluminum and copper plotted versus electron density, for a temperature of 10 000 kK. For this graph, mass data were converted to electron density using the Thomas-Fermi ionization state model of More [12].

V. DISCUSSION

In the analysis, we have assumed that the plasma fills the column uniformly, for which the only direct evidence is the symmetry and reproducibility of the photographic recordings. The water tamper resists expansion of the plasma col-

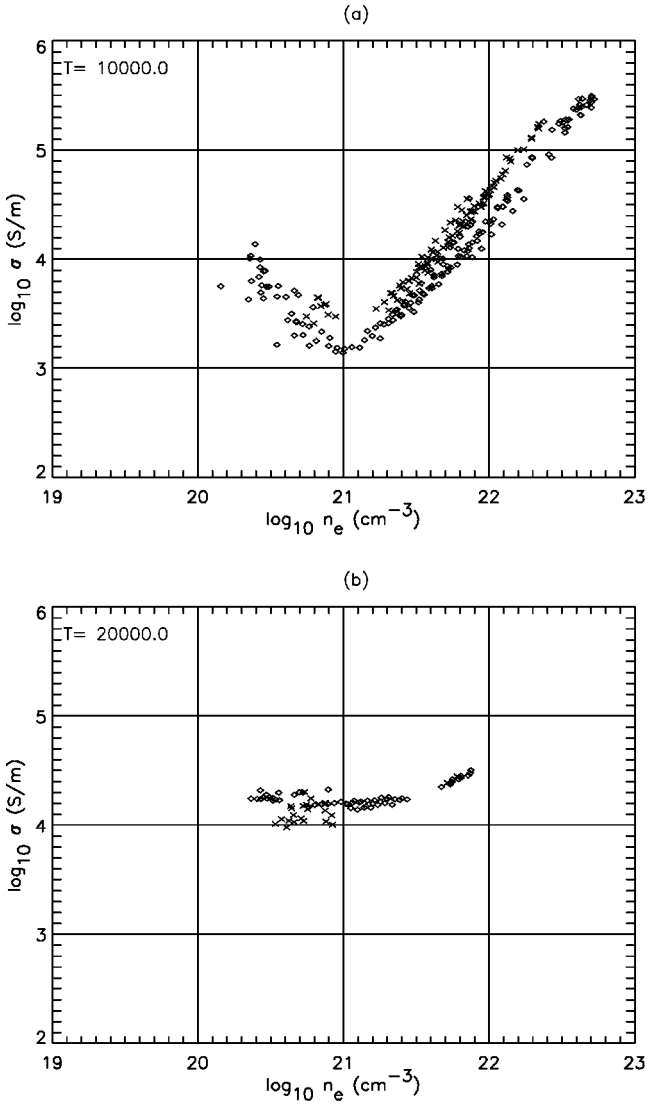

FIG. 7. Comparison of copper (diamonds) and aluminum (×'s) conductivities, plotted vs electron density. Ionization state for conversion of mass density to electron density was taken from a Thomas-Fermi model of More [12].

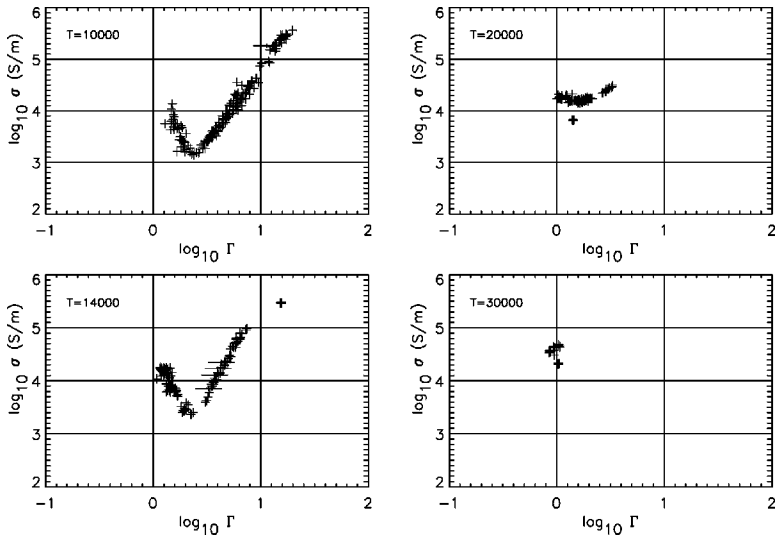

FIG. 8. Copper conductivity data plotted as a function of the coupling parameter.

umn, so that the expansion rate is always less than sound speed in the plasma. Estimates of the sound speed show that it is always greater than the expansion speed by a factor of at least 1.5. Since any radial pressure variations within the column will tend to equalize at the sound speed, we expect such variations to be small.

One must consider that under conditions where the conductivity is a strongly increasing function of temperature, a filamentation instability might arise, with current tending to concentrate in higher temperature, lower density filaments. Growth of such instabilities would be inhibited by inertia (the plasma expansion resulting from heating if pressure remains uniform), radial thermal conduction, and radiative transport, and by the inductive effects associated with modifying the current density pattern. Filamentation instabilities have been studied in connection with astrophysical and fusion plasma confinement problems, but these studies have been for conditions where magnetic fields play an important part [13], or for which conductivity is constant [14], which would not be the case in the present work. In support of our assertion of uniformity, we note that during the initial expansion phase of our discharges, the conductivity is only weakly temperature dependent, and that later, when the density is lower and the temperature dependence becomes strong, the heating rates are typically low.

The question of uniformity of a liquid metal in the near-critical state, formed by rapid Ohmic heating in a water bath, was raised by Koval', Krivitskii, and Rakovskii [15], who were able only to conclude that it should be possible to obtain valid information on the physical characteristics of the state by this method. We conclude, like those authors, that the question deserves further study, but that the assumption of uniformity appears to be a reasonable one.

The conductivity at fixed temperature seen in the present work falls more steeply with decreasing density than that reported in I, which was derived from the glass capillary shots. The two sets of data agree only at the highest densities. We suggest that the data taken in a water bath are more reliable, and that the discrepancy is in part due to the finite time required in the work reported in I for the metal vapor to fully fill the glass capillary after vaporization begins as pressure is building up. Typically this takes 300 or more ns. Previous low temperature data were derived from results during this interval, and thus may have been influenced by nonuniform density or even incompletely vaporized material in the plasma volume. In the case of the water shots, the plasma is bounded by water from the beginning, and there is no such period of uncertainty about density. A further criticism of glass confinement stems from the less-than-ideal cylindrical boundary formed by the glass. We observed in streak camera pictures in I that the glass fractured close behind the cylindrical shock wave. This would have formed fissures in the glass into which plasma could seep, causing the density to depart from that computed with the one-dimensional compression model.

In I, we showed that for values of the coupling parameter Γ approaching 100, the conductivity appeared to become a function of Γ only. The data of the present work cover the range of $1>\Gamma>20$, and do not support that conclusion in this range. In Fig. 8, we show copper data for 10 and 20 kK plotted as a function of Γ, again utilizing the ionization state in the model described by More [12]. No simple dependence of conductivity on Γ is seen, although at the largest values of Γ it appears that the conductivity may be approaching the $\sigma(\Gamma)$ dependence noted in I.

The data are compared in Figs. 5. and 6 with theoretical models for conductivity due to Ebeling *et al.* [16], Lee and More [17], Ichimaru and Tanaka [18], and Kurilenkov and Valuev [19]. The minimum in conductivity is seen only in the work of Ebeling *et al.* In the case of Ref. [18], the theory is given in the form of a fitting formula that is only valid for $\Gamma<2$ and for degeneracy parameter $Q\geqslant 0.1$ [$Q=8\pi^2 mkT/h^2(3\pi^2 n_e)^{2/3}$].

The electrical measurements of voltage and current are quite reproducible, but may have systematic errors estimated to be $\pm 5\%$. The crosses in Figs. 5 and 6 indicate an estimate of the error due to this source.

The plasma radius may be measured from the streak pictures, and is also calculated from the expansion model. An error in the column radius is reflected in both the density and conductivity, correlated in such a manner that a positive er-

ror in radius produces a reduction in both computed density and conductivity, and vice versa. The slanted error bars on selected data points in Fig. 5 and 6 indicate the effect of the error in radius. The magnitude of the error was computed as the rms difference between the computed radius of a typical shot, and that measured from the streak picture. Errors are relatively smaller when the column radius is large.

Our temperatures are deduced from the relation between energy input and temperature given in the SESAME equation of state tables. The regions of interest to our work (densities from $0.01-1\,\mathrm{g/cm^3}$, temperatures from 10–30 kK) were derived in these tables from Monte Carlo calculations for the liquid metal-to-dense gas regime, and from a Saha model for the ionized regime [20]. Unfortunately, much of our work falls in the region where neither of the two models is adequate and where the SESAME tables interpolate between them. This makes it difficult to estimate the error in temperatures. A systematic error of $\pm 30\%$ in temperature is not excluded.

We have examined the possibility that the minimum in conductivity versus density signals the metal-nonmetal transition point. According to Likalter [21], this transition occurs when the relation

$$(R_a/R_s)^3 \approx \tfrac{1}{3} \tag{3}$$

is satisfied, where $R_a = e^2/I$, I is the ionization potential, and R_s is the Wigner-Seitz radius

$$R_s = (4\pi n_i/3)^{-1/3}. \tag{4}$$

This relation is independent of temperature, but the transition presumably occurs at temperatures near the critical point. Analyzing our data for the case of copper at 8000 K, the minimum occurs at a density of about $1.2\times 10^2\ \mathrm{cm^{-3}}$, so $(R_a/R_s)^3 = 0.32$, which satisfies the relation remarkably well. In the case of aluminum, the minimum was not identified at 8000 K, but at 10 000 K is also about $1.2 \times 10^{21}\ \mathrm{cm^{-3}}$. For this case, $(R_a/R_s)^3 = 0.41$.

ACKNOWLEDGMENTS

This work was supported by the National Science Foundation. We thank David Gershon and Jeng-Mei Liu for their valuable assistance in the early stages of this work. The work would not have been possible without the expert technical help of Kenneth Diller.

[1] A. W. DeSilva and H.-J. Kunze, Phys. Rev. E **49**, 4448 (1994).
[2] L. Haar, John S. Gallagher, and G. S. Kell, *Steam Tables, Thermodynamic and Transport Properties and Computer Programs for Vapor and Liquid States of Water in SI Units* (Hemisphere, Washington, DC, 1984), p. 269.
[3] *Metals: Electronic Transport Phenomena*, edited by K.-H. Hellwege, Landolt-Bornstein, New Series, Group III, Vol. 15, Pt. X (Springer-Verlag, Berlin, 1982), p. 31.
[4] *Specific Heat: Metallic Elements and Alloys*, edited by Y. S. Touloukian, Thermophysical Properties of Matter Vol. 1 (IFI/Plenum, New York, 1967), p. 456.
[5] *Thermal Expansion: Metallic Elements and Alloys*, edited by Y. S. Touloukian *et al.*, Thermophysical Properties of Matter Vol. 12, (IFI/Plenum, New York, 1970), p. 77.
[6] T. Iida and R. I. L. Guthrie, *The Physical Properties of Liquid Metals* (Clarendon, Oxford, 1988).
[7] SESAME: The Los Alamos National Laboratory Equation of State Database, Report No. LA-UR-92-3407, edited by S. P. Lyon and J. D. Johnson, Group T-1 (unpublished).
[8] M. N. Plooster, Phys. Fluids **13**, 2665 (1970).
[9] M. H. Rice and J. M. Walsh, J. Chem. Phys. **26**, 824 (1957).
[10] H. Reinholtz, R. Redemer, and S. Nagel, Phys. Rev. E **52**, 5368 (1995).
[11] W. Götzlaff, G. Schönherr, and F. Hensel, Z. Phys. Chem., Neue Folge **156**, 219 (1988).
[12] R. M. More, in *Handbook of Plasma Physics*, edited by M. N. Rosenbluth and R. Z. Sagdeev, Physics of Laser Plasma, Vol. 3 (Elsevier, Amsterdam, 1991), p. 70.
[13] J. F. Drake, L. Sparks, and G. Van Hoven, Phys. Fluids **31**, 813 (1988).
[14] G. S. Murty, Ark. Fys. **18**, 241 (1960).
[15] S. V. Koval', E. V. Krivitskii, and G. B. Rakovskii, Zh. Tekh. Fiz. **61**, 61 (1991) [Sov. Phys. JETP **36**, 756 (1991)].
[16] W. Ebeling, A. Förster, V. Fortov, V. Gryaznov, and A. Polishchuk, *Thermophysical Properties of Hot Dense Plasmas*, Teubner-Texte zur Physik Vol. 25 (Teubner Verlagsgesellschaft, Stuttgart, 1991), pp. 274–275.
[17] Y. T. Lee and R. M. More, Phys. Fluids **27**, 1273 (1984).
[18] S. Ichimaru and S. Tanaka, Phys. Rev. A **32**, 1790 (1985).
[19] Yu. K. Kurilenkov and A. A. Valuev, Beitr. Plasmaphys. **24**, 161 (1984).
[20] K. S. Trainor, J. Appl. Phys. **54**, 2372 (1983).
[21] A. Likalter, Phys. Scr. **55**, 114 (1997).